Desalination and Water Treatment
www.deswater.com

doi: 10.5004/dwt.2019.23843

149 (2019) 288–294
May

Influence of mine drainage on regional groundwater of Shilou iron mine in Huaibei City, Anhui Province, China

Jie Yang[a,*], Pengqiang Cao[b], Yulan Gao[a], Rusheng Jia[a], Youxiao Tu[a], Yuezan Tao[c]

[a]*Department of Architecture and Civil Engineering, West Anhui University, Liu'an 237012, China, email: yangjie6363@163.com (J. Yang)*
[b]*Anhui & Huai River Institute of Hydraulic Research, Bengbu 233000, China*
[c]*School of Civil and Hydraulic Engineering, Hefei University of Technology, Hefei 230009, China*

Received 22 October 2018; Accepted 15 January 2019

ABSTRACT

When mining in mines, it is inevitable to produce water gushing; the influence of large amount of mine drainage on groundwater is a problem that should be taken seriously. Taking Shilou Iron Mine for example, based on regional hydrogeological concept model, the numerical model of groundwater was established, which was identified by water-level simulation and crossflow rate calculation, and then the additional drawdown hydrograph was analyzed by considering whether there was water bursting. The results showed that the maximum drawdown of water level of karst water aquifer in the mining area was 0.2753 and 0.2662 m when considering two months of water inrush and normal water gushing by the end of the third year. In addition, the area where groundwater drawdown was greater than 0.2 m was within the radius of 1,500 m at the center of the pit mine, and the mine drainage was of some influence on regional karst groundwater. Furthermore, the maximum value of pore water aquifer was 0.0126 and 0.0104 m in the same case, and the drawdown funnel was roughly stable, so it had little influence on regional pore groundwater during the study period.

Keywords: Water gushing; Numerical simulation; Groundwater drawdown; Crossflow rate; Mine drainage; Pore water aquifer

1. Introduction

The water gushing in mine pit refers to groundwater which flows into the mine through various roadways and mining systems during the construction and production of mines [1]. In recent years, there were frequent occurrences of mine accidents due to water inrush which not only brought huge economic losses to the country but also devoured the lives of many miners [2–4]. Therefore, it is necessary to carry out related research on water bursting and drainage in mine pit. Many scholars at home and abroad have done a lot of research on this topic and achieved some results [5–7]. For example, the tectonic mechanism of water inrush in karst area from the perspective of water storage model, and a corresponding prediction method for water inflow was put forward [8]. Some researchers used discrete element method and software PFC3D to establish a 3D numerical model of water burst in the deep tunnel [9]. A group of researchers established Bayesian discrimination model, fuzzy discrimination model, and gray discrimination model based on water chemical information and obtained the optimum model of water inrush by comparing with the actual water samples [10]. Some researchers predicted the inflow and radius of influence of an open pit mine based on the empirical model and analytical model and analyzed the groundwater recovery after mining [11]. Others researchers used SEEP/W finite element software to establish a numerical model for a mine in Iran, predicted the groundwater runoff and compared with the actual observed data; other researchers discussed the effect of certain acid mine drainage in eastern Turkey

* Corresponding author.

1944-3994/1944-3986

on the surrounding groundwater, and analyzed the possible influence on the soil, sediment, plant and surface water of the mining area [12,13].

Much of the research had focused on the forecast of water gushing, mechanism of water inrush, assessment and prevention of water burst, effect of mine drainage on water quality, but there were few concerns about the influence of drainage on groundwater level in the mining area [14–23]. Based on the above questions, this paper took Shilou Iron Mine as an example, started from the regional hydrogeological concept model, used the Visual Modflow software to establish numerical model, and carried out the water-level simulation and crossflow rate calculation. What's more, the additional drawdown hydrographs of karst water and pore water aquifer were analyzed and then the impact on groundwater in certain area was determined through the changing trend of water level.

2. Materials and methods

2.1. Study area

Shilou Iron Mine is located in Suixi County of Huaibei which is a city in Eastern China, and the geomorphologic type is alluvial plain, and ground elevation is about 28.5–29.9 m. The Paleozoic strata development in the region mainly includes the Middle Ordovician and the loose Quaternary strata; among them, the Ordovician limestone karst fissure water is the main water source in Huaibei city. Additionally, regional water sources in eastern and western are 0–80 and 30–60 m, respectively. According to the lithologic combination of aquifer medium, times, and water-bearing characteristics, the study area can be divided into three aquifers which are Quaternary pore phreatic water, Carboniferous, and Ordovician karst fissure confined aquifer from top to bottom; a relatively stable layer of clay is isolated between pore phreatic water and fissure karst water, which makes the hydraulic connection weak.

2.2. Numerical simulation of groundwater

2.2.1. Hydrogeology conceptual model

In the simulation of groundwater flow system in mining area, first the regional hydrogeological conceptual model needs to be established, and the model is an approximate treatment of the actual complex system, which is connected with the numerical model through reasonable generalization. The simulation range is mainly divided along the boundary between the Carboniferous and Permian strata; the east-west span is about 10.35 km and north-south is about 16.25 km, a total area of approximately 167.5 km^2. Second, when the boundary of the model is setup, the change in regional stratigraphic lithology ought to be taken into consideration; the northern part is generalized to the boundary of fixed water level, and others are impermeable. Furthermore, according to the distance from Shilou Iron Mine to Suixi Waterworks which is about 7.5 km, it can set four representative points in between which are point 1, point 2, point 3, and point 4; each point distance from the center of the mining area is 1,500, 3,000, 5,000, and 7,500 m, respectively. Therefore, the effect of drainage on the groundwater in the mining area is reflected by the change of drawdown of water level in every point. The location distribution of the points is shown in Fig. 1.

2.2.2. Mathematical model

According to the generalized hydrogeological conceptual model, the regional subsurface water is generalized into the non-homogeneous, anisotropic, and unstable groundwater flow system, and the corresponding numerical simulation mathematical model is established as follows:

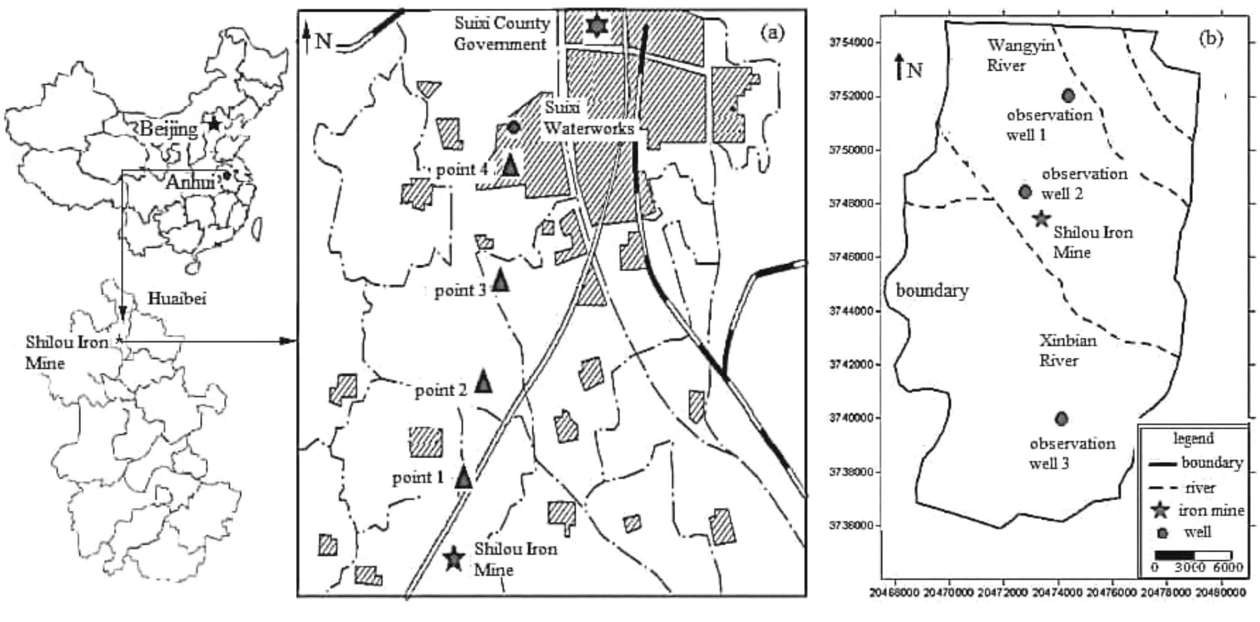

Fig. 1. The location distribution of the representative points and water-level observation wells of the research area. (a) Distribution of the representative points and (b) distribution of the observation wells.

$$\frac{\partial}{\partial x}\left(KM\frac{\partial H}{\partial x}\right)+\frac{\partial}{\partial y}\left(KM\frac{\partial H}{\partial y}\right)+\frac{\partial}{\partial z}\left(KM\frac{\partial H}{\partial z}\right)+W=\mu^*\frac{\partial H}{\partial t} \quad (1)$$

$$H(x,y,z,t)\big|_{t=0}=H_0(x,y,z) \qquad (x,y)\in D \quad (2)$$

$$H(x,y,z,t)\big|_{\Gamma_1}=H_1(x,y,z,t) \qquad (x,y)\in \Gamma_1 \quad (3)$$

$$KM\frac{\partial H}{\partial n}\Big|_{\Gamma_2}=0 \quad (4)$$

2.2.3. Dispersion of time and space

In terms of time, January 2009 was the initial time for simulation; the period was from January 2009 to December 2011, and the calculation step was one month, and then the average water level of each point was calculated month by month, so the model could be identified by comparing the calculated values with the observed values. In space, the study area was divided into 150 rows and 100 columns in the plane, with a total of 15,000 cells. It was divided into three layers which represent the phreatic aquifer, confined aquifer, and fractured karst confined aquifer from top to bottom.

2.2.4. Observation wells and mining wells

According to the preliminary exploration and the hydrogeological survey, there are three observation wells of water level in the simulation range for which distribution is shown in Fig. 1(b). The fractured karst water mining wells in this project are mainly located in the urban areas of Suixi and mining, for which the annual production are 2,361.72 × 10^4 and 153.07 × 10^4 m^3 $d^{-1,}$ respectively. By the regional water surveying, the annual total excavation volume is approximately 914.14 × 10^4 m^3 d^{-1}, which is generalized to two mining wells.

3. Results

3.1. Model identification

3.1.1. Simulation of water level

The parameters were adjusted repeatedly through the method of trial and error; finally, an ideal model identification result was obtained which is shown below [24–26]. Fig. 2 shows the comparison of the calculated water level with observation water level at the end of 2009. It could be seen from the diagram that the average error of groundwater level between model simulation and actual observation was 0.183 m, for which the mean square root was 0.318 m. Figs. 3(a)–(c) are the correlation curves of water level between the calculated and the observed values of the observation wells 1, 2, and 3, respectively.

3.1.2. Calculation of crossflow rate

The actual mine drainage was 0.2 × 10^4 – 0.4 × 10^4 m^3 d^{-1}, and it was 0.4 × 10^4 m^3 d^{-1} when analyzed in the process of model prediction. Considering the pit water bursting, the drainage for the first two months was 3.0 × 10^4 m^3 d^{-1}; the stage hydrograph and crossflow rate before and after mine drainage are shown in Fig. 4(a) and Table 1 [27]. By analysis of hydrograph, it could be seen that mine drainage had a very small influence on pore groundwater; the variation of crossflow rate in the first year was relatively large which was mainly caused by the water bursting [28–30]. As the difference in water level is very small, the stage hydrograph is enlarged in the first six months, as is shown in Fig. 4(b).

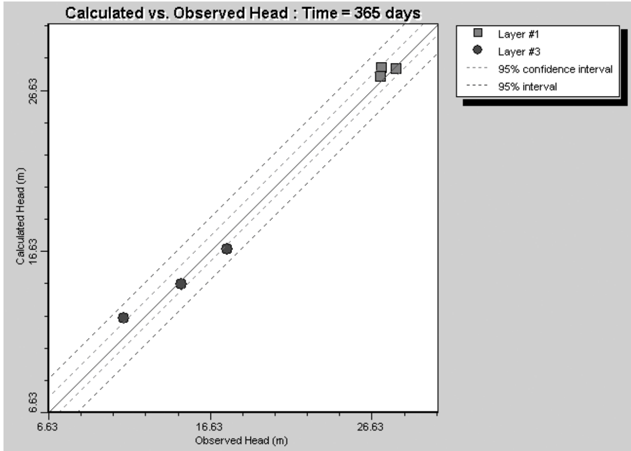

Fig. 2. The scatter plot of calculated water level and observed water level.

3.2. Analysis of numerical solution

3.2.1. Analysis on the drawdown of water level during water bursting

For the karst aquifers, it can calculate the additional drawdown of water level of each representative points at different times when the mine drainage continues to the 3, 6, 12, 24, and 36 months [31–34]. For the upper porous aquifer, according to the drawdown of central pit and karst water in the third year (1,095 d), it can also get the value of porous aquifer caused by crossflow. In consideration of water bursting, the iron mine was drained at 30,000 m^3 d^{-1} in the first two months and then pumped at 4,000 m^3 d^{-1} which was on the basis of actual water drainage; the calculated results are shown in Table 2, Figs. 5(a) and (b).

According to the above chart, under the condition of water inrush in two months, the maximum additional drawdown of water level of karst water was 0.501 m in the center of mining area; about 6 months later, the drawdown of all points had a decreasing trend. In addition, by the end of the third year, the additional drawdown hydrograph of karst water was basically stable, for which the value of all points beyond the radius of 1,500 m was not greater than 0.2 m, and the maximum drawdown in the karst water source of Suixi Waterworks was 0.12 m (about 181 d), so the mine drainage did not affect normal water source during the study period. Furthermore, the maximum drawdown of pore water was 0.0126 m, and all the points except 1 were less than 0.01 m, so the effect on regional groundwater was very limited, and the drawdown funnel was also roughly stable after 3 y [35,36].

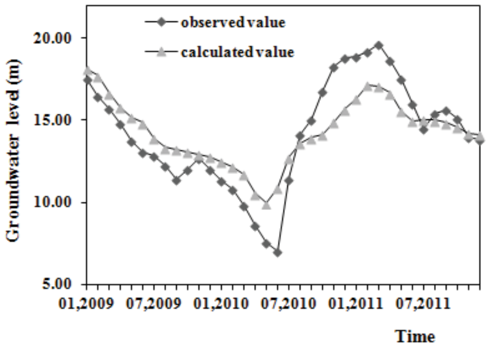

(a) The curve of water level in well 1

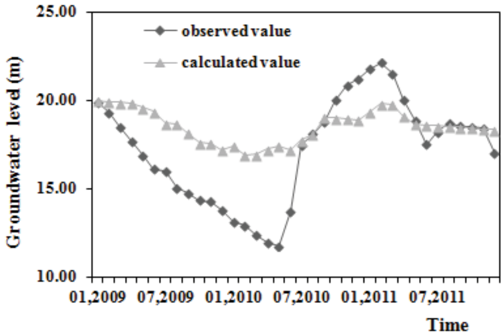

(b) The curve of water level in well 2

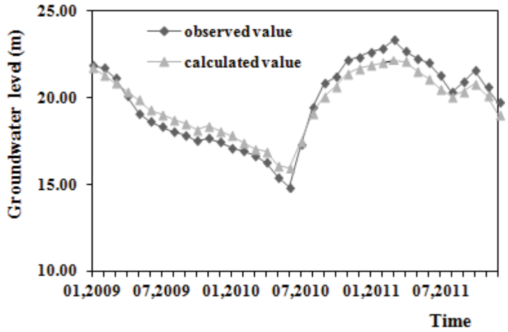

(c) The curve of water level in well 3

Fig. 3. The correlation curve of calculated water level and observed water level in observation wells 1, 2, and 3.

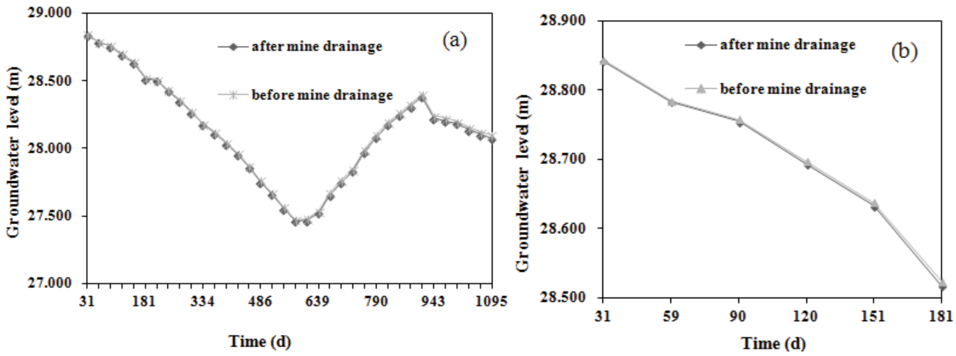

Fig. 4. The hydrograph of water level before and after mine drainage. (a) The hydrograph in 1,095 d and (b) the hydrograph in 181 d.

Table 1
The crossflow rate calculation of mine drainage

Year	Pre-drainage value ($\times10^4$ m^3 a^{-1})	Drainage value ($\times10^4$ m^3 a^{-1})	Variation value ($\times10^4$ m^3 a^{-1})	Rate of change (%)
2009	582.30	594.86	12.56	2.16
2010	690.96	699.89	8.93	1.29
2011	580.85	588.97	8.12	1.40

3.2.2. Analysis on the drawdown of water level without water bursting

When the sudden rushing of water was not taken into account, the actual water flow of Shilou Iron Mine was pumped by the drainage of 4,000 m^3 d^{-1}; the additional drawdown of water level on the regional karst water and pore water is shown in Table 3 and Figs. 6(a) and (b).

Combining the above diagrams, when considering without water bursting, the initial drawdown of water level of karst water was 0.115 m in the center of the mining area; it reached the maximum of 0.272 m by the 1,095th day, and the value of rest points were simultaneously increasing, but the trend of drawdown hydrograph had leveled off later. Besides, the drawdown of the pore water level was lower at

Table 2
The drawdown of water level of karst water and pore water at the end of three years. (with water bursting)

Representative points	Distance from pit center (m)	Drawdown of karst water (m)	Drawdown of pore water (m)
Center of pit	0	0.2753	0.0126
Point 1	1,500	0.2002	0.0125
Point 2	3,000	0.1399	0.0096
Point 3	5,000	0.0772	0.0060
Point 4	7,500	0.0182	0.0025

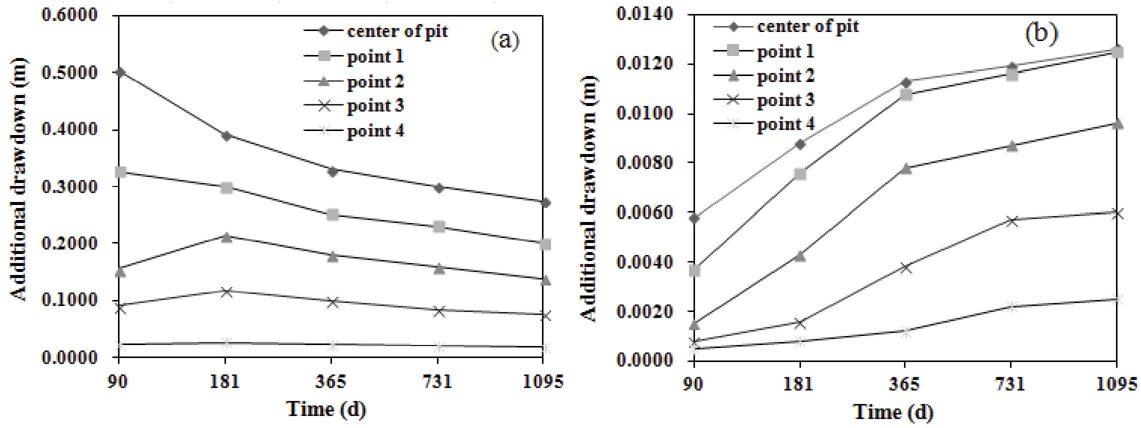

Fig. 5. The additional drawdown (a) hydrograph of karst water and (b) pore water with water bursting.

Table 3
The drawdown of water level of karst water and pore water at the end of three years (without water bursting)

Representative points	Distance from pit center (m)	Drawdown of karst water (m)	Drawdown of pore water (m)
Center of pit	0	0.2662	0.0104
Point 1	1,500	0.1917	0.0102
Point 2	3,000	0.1330	0.0076
Point 3	5,000	0.0735	0.0044
Point 4	7,500	0.0174	0.0018

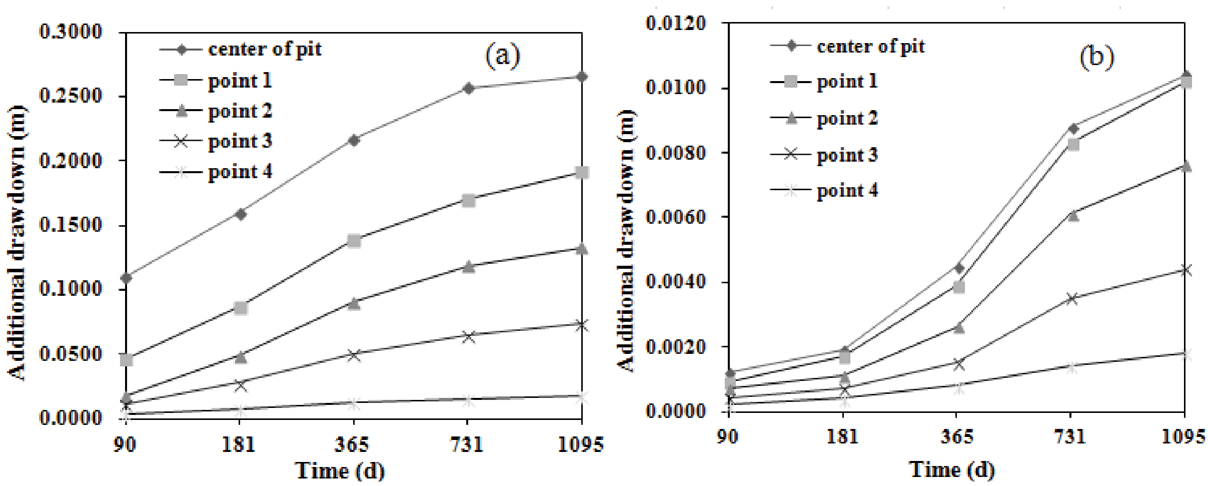

Fig. 6. The additional drawdown (a) hydrograph of karst water and (b) pore water without water bursting.

the starting point which was about 0.001 m, and the value of every point had increased significantly over the past 3 y, for which the maximum was approximately 0.01 m. Although the value of pore water had increased a lot, it had a lower base, and due to the stable clay layer isolation between pore water and karst water, the pore water was less affected by the mine drainage.

4. Discussion and conclusions

Through the simulation study on mine drainage of Shilou, the following conclusions can be drawn.

- When numerical method was to analyze mine drainage, the premise of which was simulation of groundwater flow field, based on the generalized regional hydrogeological conceptual model, the corresponding numerical model was established, the time space dispersion and distribution of wells should be considered. Second, by applying Visual Modflow software, the results of model recognition were mainly achieved by comparing calculated value and observed value with the observation wells.
- Distinguishing whether water inrush or not, the drawdown of water level in the aquifer of karst water and pore water was calculated and analyzed the trend of additional drawdown hydrograph of them in the above two cases. By the end of the third year, the karst water drawdown was basically stable, which in pit center was 0.2753 and 0.2662 m, respectively, in the occurrence of water bursting and normal water gushing. What's more, there was a rising trend of drawdown of pore water, which in pit center was 0.0126 m and 0.0104 m, respectively, in the same case, but the late hydrograph is roughly flat, it had a limited impact on regional groundwater during the calculation period.
- There were many "large mining wells" in the study area such as the drainage of Shilou and Liuqiao Mine, the current situation and planning exploration of water source in Suixi Waterworks, and the influence of these well groups on the regional groundwater level was mutual interference, which was not fully considered in the article, so the accuracy of numerical results would be affected. Additionally, in the longer study period, how to combine the surface water ecosystem to analyze the change law of the regional underground flow field will carry out further research in the later work.

Symbols

D — The simulation area
H — The groundwater level, m
H_0 — The initial water level of groundwater, m
H_1 — The groundwater level at the simulated boundary, m
K — The aquifer hydraulic conductivity, m d^{-1}
M — The thickness of confined aquifer, m
t — Time, d
W — The unit volume flow, m^3
Γ_1 — The first-class boundary of head loss
Γ_2 — The second type of flowrate boundary
μ^* — The elastic storage coefficient

Acknowledgements

This research work was supported by the key project of Natural Science Foundation of Anhui (Grant No. KJ2017A409), partly supported by the National Natural Science Foundation of China (Grant No.51309071) and Supported by Natural Science Foundation of West Anhui University (Grant No. WXZR201618).

References

[1] S.S. Zheng, J.Z. Cheng, H.H. Liu, Specialized Hydrogeology, China University of Mining and Technology Press, Xuzhou, 1999.
[2] D.T. Allen, D.J. Carrier, J. Gong, B. Hwang, P. Licence, A. Moores, T. Pradeep, B. Sels, B. Subramaniam, M.K.C. Tam, L. Zhang, R.M. Williams, Advancing the use of sustainability metrics in ACS sustainable chemistry and engineering, ACS Sustainable Chem. Eng., 6 (2018) 1.
[3] F.F. Bobinihi, J. Osuntokun, D.C. Onwudiwe, Syntheses and characterization of nickel(II) dithiocarbamate complexes containing NiS_4 and NiS_2PN moieties: nickel sulphide nanoparticles from a single source precursor, J. Saudi Chem. Soc., 22 (2018) 381–395.
[4] A.A.P. Khan, A. Khan, A.M. Asiri, S.A. Khan, A. Mohd, Complexation and oxidation of Flutamide with Fe^{3+} and 1,10-phenanthroline: few analytical applications, Arabian J. Chem., 11 (2018) 240–246.
[5] W. Gao, W. Wang, A tight neighborhood union condition on fractional (g, f, n', m)-critical deleted graphs, Colloq. Math. Warsaw., 149 (2017) 291–298.
[6] D. Li, L. Wang, W. Peng, S. Ge, N. Li, Y. Furuta, Chemical structure of hemicellulosic polymers isolated from bamboo biocomposite during mold pressing, Polym. Compos., 38 (2017) 2009–2015.
[7] W. Peng, S. Ge, A.G. Ebadi, H. Hisoriev, M.J. Esfahani, Syngas production by catalytic co-gasification of coal-biomass blends in a circulating fluidized bed gasifier, J. Cleaner Prod., 168 (2017) 1513–1517.
[8] C.N. Lin, L.P. Li, X.R. Han, Research on forecast method of tunnel water inrush in complex karst areas, Chinese J. Rock Mech. Eng., 27 (2008) 1469–1476.
[9] Y. Wang, Y.G. Lu, X.D. Ni, D.T. Li, Study on mechanism of water burst and mud burst in deep tunnel excavation, J. Hydraul. Eng., 42 (2011) 595–601.
[10] X.M. Wang, X.P. Zhou, Y. Liu, J.Z. Qian, Optimum discrimination model of water-inrush source based on water chemical information in Gubei coal mine, Saf. Environ. Eng., 20 (2013) 122–125.
[11] Y. Yihdego, A. Paffard, Predicting open pit mine inflow and recovery depth in the durvuljin soum, Zavkhan Province, Mongolia, Mine Water Environ., 36 (2017) 114–123.
[12] S. Bahrami, F. Doulati Ardejani, S. Aslani, E. Baafi, Numerical modelling of the groundwater inflow to an advancing open pit mine: Kolahdarvazeh pit, Central Iran, Environ. Monit. Assess., 186 (2014) 8573–8585.
[13] M.I. Yesilnacar, Z. Kadiragagil, Effects of acid mine drainage on groundwater quality: a case study from an open-pit copper mine in eastern Turkey, Bull. Eng. Geol. Environ., 72 (2013) 485–493.
[14] C.P. Liu, C.C. Zheng, Analysis and simulate of mine water inflow in Anqing copper mine, Geotech. Invest. Surv., 1 (2000) 3–6.
[15] X. Zhou, X.Y. Zhu, C.Y. Wen, S. Chen, Application of ANN to predict the drainage in mine, J. Hydraul. Eng., 12 (2000) 59–63.
[16] L.P. Li, S.C. Li, Q.S. Zhang, Study of mechanism of water inrush induced by hydraulic fracturing in karst tunnels, Rock Soil Mech., 31 (2010) 523–528.
[17] Y. Manawi, A.K. Fard, M.A. Hussien, A. Benamor, V. Kochkodan, Evaluation of the current state and perspective of wastewater treatment and reuse in Qatar, Desal. Wat. Treat., 71 (2017) 1–11.

[18] Z.W. Liu, M.C. He, S.R. Wang, Study of karst waterburst mechanism and prevention countermeasures in Yuanliangshan tunnel, Rock Soil Mech., 27 (2006) 228–232.

[19] C. Sena, J. Molinero, Water resources assessment and hydrogeological modelling as a tool for the feasibility study of a closure plan for an open pit mine (La Respina Mine, Spain), Mine Water Environ., 28 (2009) 94–101.

[20] U. Gemici, Impact of acid mine drainage from the abandoned Halikoy Mercury mine (western Turkey) on surface and groundwaters, Bull. Environ. Contam. Toxicol., 72 (2004) 482–489.

[21] J.S. Kuma, P.L. Younger, W.K. Buah, Numerical indices of the severity of acidic mine drainage: broadening the applicability of the gray acid mine drainage index, Mine Water Environ., 30 (2011) 67–74.

[22] J. Gonzalez-Trinidad, H.E. Junez-Ferreira, A. Pacheco-Guerrero, E. Olmos-Trujillo, C.F. Bautista-Capetillo, Dynamics of land cover changes and delineation of groundwater recharge potential sites in the aguanaval aquifer, Zacatecas, México, Appl. Ecol. Environ. Res., 15 (2017) 387–402.

[23] R. Strachel, J. Wyszkowska, M. Bacmaga, The effect of nitrogen on the microbiological and biochemical properties of zinc-contaminated soil, J. Environ. Eng. Landscape Manage., 25 (2017) 13–22.

[24] L.C. Shu, Y.F. Tao, P.G. Liu, Reliability calculation method for groundwater recharge in consideration of uncertainty of hydrogeological parameters, J. Hydraul. Eng., 39 (2008) 346–350.

[25] R. Pessoa, L. Pereira, R.C. Sousa, R.M. Costa, Water quality during the recreational high season for a macrotidal beach (Ajuruteua, Para, Brazil), J. Coastal Hazards, 752 (2016) 1222–1226.

[26] X. Shi, Y. Liu, Y. Tang, L. Feng, L. Zhang, Kinetics and pathways of Bezafibrate degradation in UV/chlorine process, Environ. Sci. Pollut. Res., 25 (2018) 672–682.

[27] W.T. Chen, M.N. Wang, L.H. Wei, Y.L. Ji, Z.Y. Gai, R.D. Huang, Analysis of causes and disposals for water gushing of land regions Xiamen of submarine tunnel, Chin. J. Geotech. Eng., 30 (2008) 457–461.

[28] L.P. Li, S.S. Shi, S.C. Li, Z.H. Xu, Z.Q. Zhou, Comprehensive prediction of fissure water in extra-long deep tunnel and its application, Chin. J. Underground Space Eng., 9 (2013) 603–609.

[29] J.Z. Qian, G.Y. Pan, J.F. Wu, X.X. Zhu, Mechanism of preferential flow in the media of fractured karst in Jiaozuo Mine, J. Hydraul. Eng., 34 (2003) 95–99.

[30] X.H. Xie, B.Y. Su, Y.F. Gao, X.B. Duan, Numerical study on water inrush above a confined aquifer in coal mining using hydro-fracturing. Chin. J. Rock Mech. Eng., 24 (2005) 987–993.

[31] M.M. Parvez, M.M. Billah, M.M. Iqbal, M.M. Rahman, M.K.A. Bhuiyan, S.S. Romkey, M.A.O. Dawood, M.S. Islam, Fish diversity and water characteristics in the Reju Khal River, Water Conserv. Manage., 2 (2018) 11–19.

[32] L. Yang, H. Guo, H. Chen, L. He, T. Sun, A bibliometric analysis of desalination research during 1997–2012, Water Conserv. Manage., 2 (2018) 18–23.

[33] K. Kadharsha, S.A. Khan, S. Lyla, P. Mohanchander, A. John, Checklist for commercially important food fishes of Parangipettai, Southeast Coast of India, J. CleanWAS, 2 (2018) 16–19.

[34] A.R.M. Firdaus, M.A.A. Samah, K.B.A. Hamid, Chns analysis towards food waste in composting, J. CleanWAS, 2 (2018) 6–10.

[35] A. Rafiq, A. Rasheed, C. Arslan, U. Tallat, M. Siddique, Estimation of greenhouse gas emissions from Muhammad wala open dumping site of Faisalabad, Pakistan, Geol. Ecol. Landscapes, 2 (2018) 45–50.

[36] T.D.T. Oyedotun, A.R. Luna, A.G.N. Hernández, Contemporary shoreline changes and consequences at a tropical coastal domain. Geol. Ecol. Landscapes, 2 (2018) 104–114.